Geophysical Research Letters

RESEARCH LETTER
10.1029/2020GL089740

Radiosonde Observations of a Wintertime Meridional Convergence of Gravity Waves Around 60°S in the Lower Stratosphere

T. Moffat-Griffin[1], S. R. Colwell[1], C. J. Wright[2], N. P. Hindley[2], and N. J. Mitchell[2]

[1]Atmosphere, Ice and Climate Team, British Antarctic Survey, Cambridge, UK, [2]Centre for Space, Atmospheric and Oceanic Science, University of Bath, Bath, UK

Key Points:
- This paper provides evidence of a winter time convergence of gravity waves and their momentum flux toward 60°S
- This is the first time this has been observed for short vertical wavelength waves in the lower stratosphere

Supporting Information:
- Supporting Information S1

Correspondence to:
T. Moffat-Griffin,
tmof@bas.ac.uk

Citation:
Moffat-Griffin, T., Colwell, S. R., Wright, C. J., Hindley, N. P., & Mitchell, N. J. (2020). Radiosonde observations of a wintertime meridional convergence of gravity waves around 60°S in the lower stratosphere. *Geophysical Research Letters*, *47*, e2020GL089740. https://doi.org/10.1029/2020GL089740

Received 10 AUG 2020
Accepted 19 SEP 2020
Accepted article online 22 SEP 2020

Abstract Satellite observations show that there is a wintertime hotspot of gravity wave activity, located mainly over the ocean, around 60°S in the stratosphere. However, the sources of the gravity waves making up this hotspot are varied and complex and remain unclear. Here we use radiosonde observations from 11 Antarctic stations and selected small islands close to 60°S to examine the horizontal directional pseudo-momentum flux and energy density distributions of upward propagating gravity waves in the lower stratosphere. This paper shows, for the first time, that short vertical wavelength gravity waves in the lower stratosphere clearly propagate meridionally toward 60°S during the winter months. This result supports previous studies that show that this belt of gravity wave activity over the ocean is contributed to by wave sources outside 60°S.

Plain Language Summary Atmospheric gravity waves are buoyancy waves, where the restoring force is gravity, which can have horizontal wavelengths from a few tens to hundreds of kilometers. They can be generated by a variety of sources including wind flow over mountains and storms. Over the Drake Passage and out to the east around 60°S, a large hotspot of gravity waves has been observed in the wintertime stratosphere using satellite observations. The sources for this gravity wave hotspot are unclear as it mainly located over the open ocean. In this paper radiosonde observations are used to examine, for the first time, the directional variation in short vertical wavelength gravity waves close to 60°S in the lower stratosphere. It is found that during the winter months there is a meridional convergence of gravity waves toward 60°S, implying that the gravity wave sources of the hotspot are in fact be outside this region.

1. Introduction

Atmospheric gravity waves are buoyancy waves where the restoring force is gravity and are ubiquitous throughout the atmosphere. These waves can be generated by a range of sources including wind flow over mountains (orographic waves), the Polar Vortex, storms, and geostrophic adjustment (Fritts & Alexander, 2003). Gravity waves are one of the most important mechanisms of transporting energy and momentum from the troposphere to the middle and upper atmosphere. The deposition of the gravity wave energy and momentum into the mean flow can occur via a range of mechanisms, including wave breaking and critical level filtering (Fritts et al., 2006; Hoffmann et al., 2013; Whiteway & Duck, 1996). This transfer of energy and momentum means that gravity waves play a crucial role in driving global atmospheric circulation (Allen & Vincent, 1995).

By comparison to the larger global-scale waves in the atmosphere (e.g., planetary waves and tides), gravity waves are small in physical scale, with horizontal wavelengths ranging from tens to hundreds of kilometers and vertical wavelengths 2 km to tens of kilometers. Because of this, in global circulation models gravity waves are normally represented by parameterizations (Fritts & Alexander, 2003; Garcia et al., 2017; Jackson et al., 2017), as they are too small to be resolved by the coarser grid sizes used in some global models. However, it has been shown that these parametrizations underestimate gravity wave drag in the Antarctic atmosphere (Garcia et al., 2017), which results in some models having stratospheric temperatures that are too cold (the "cold pole" problem) and zonal wind speeds that are too strong in spring (Hendricks et al., 2014; Hoffmann et al., 2016; McLandress et al., 2012) relative to the observed climatology. These parameterizations need to be improved. This can be done through observations which provide information on the sources and variability of the gravity wave field.

Satellite observations show that there is a band of high gravity wave activity around 60°S during the austral winter months (M. J. Alexander, Eckermann, et al., 2009; P. Alexander et al., 2010; Hendricks et al., 2014; Hindley et al., 2015, 2019; PDC, 2015). This band stretches from a region of intense gravity wave activity over the Southern Andes and the Antarctic Peninsula and eastward over the Southern Ocean. These waves are not well represented in global circulation model parameterizations which results in "missing" momentum flux in the simulated system relative to that believed to be present in the true Earth system. The reason for this discrepancy is due to the sources of the gravity waves in this region not being well determined.

The gravity waves generated over the Southern Ocean during the austral winter are thought to be due to a combination of orographic sources (mountain ranges and isolated small islands) (M. J. Alexander & Grimsdell, 2013; Hendricks et al., 2014; Hoffmann et al., 2016; Jackson et al., 2017; Moffat-Griffin et al., 2017) and non-orographic sources such as frontal systems, jet instability, and deep convection (S. P. Alexander et al., 2016; Wu & Eckermann, 2008). However, this alone does not account for all the expected missing momentum (M. J. Alexander, Eckermann, et al., 2009; M. J. Alexander & Grimsdell, 2013; Hindley et al., 2019; Hoffmann et al., 2016). There have also been studies on "non-local" sources that can contribute to the momentum flux in this region, some studies showing that wave sources up to 10° away can contribute (S. P. Alexander et al., 2016; Hindley et al., 2015; Jiang et al., 2014, 2019; Sato, 2010).

Significant work has been done in studying this problem using satellites (M. J. Alexander & Grimsdell, 2013; S. P. Alexander, Klekociuk, & Tsuda, 2009; Hendricks et al., 2014; Hindley et al., 2015, 2019; Hoffmann et al., 2016; Wright et al., 2016; Wu & Jiang, 2002); to date only limited work has been carried out using radiosonde data. Radiosondes and satellite data sets observe different parts of the gravity wave spectrum (due to observational filtering, M. J. Alexander, 1998; Wright et al., 2016). Satellite observations, unlike radiosonde observations, cannot see the short vertical and short horizontal wavelength gravity waves. That radiosondes can access a part of the gravity wave spectrum inaccessible by satellites means that they can provide vital new information about these waves and their propagation characteristics in the lower stratosphere.

Using radiosonde data from multiple sites across the Southern Ocean region, this paper will examine the suggestion that many of the gravity waves seen close to 60°S propagate into this region. This is the first study of the horizontal direction distribution of the total energy density and absolute momentum flux of gravity waves in the lower stratosphere derived from radiosonde data taken close to 60°S.

2. Radiosonde Data

For this study high-resolution radiosonde data from 11 Antarctic/sub-Antarctic stations, with a range of data availability, were used, of which 10 launch radiosondes year round and an additional one during the summertime only. The stations selected are close to 60°S, both to the North and the South of this latitude. The selected stations are within 15° latitude of 60°S.

Table 1 lists the radiosonde data sets from Antarctic stations used in this paper. It includes station locations, the radiosonde type, and the period of data coverage studied.

For all the data there are daily launches at 11 UT. Some stations (with the exception of Kerguelen Island, Dumont D'Urville, and Princess Elisabeth station) provide additional regular launches at 23 UT or operated intensive radiosonde campaigns with multiple launches per day, and these data were also included in the analysis for this paper. The radiosondes are launched on weather balloons and rise rapidly through the atmosphere gathering vertical profiles of altitude, temperature, wind speed, pressure, wind direction, and humidity. The balloons typically burst in the lower stratosphere (~20–35 km depending on balloon type and atmospheric conditions) at which point data collection stops. In this study the focus is on the lower stratosphere, and radiosonde profiles that provide data in the altitude range 12–30 km are used. The high sampling rate of the radiosonde data means that gravity waves with very short vertical wavelengths (9 km and shorter) can be easily resolved. In comparison, satellites observations generally struggle to resolve this part of the vertical wavelength spectrum (M. J. Alexander & Barnet, 2007). This means that the radiosonde measurements provide a valuable data set of observations in a hard-to-observe part of the gravity wave spectrum.

Three different types of radiosondes were used across the stations with the most common being the Vaisala model (Vaisala, 2013). The other two types used are the Graw DFM-09 (GRAW, 2020) and the Modem M2K2-DC (MeteoModem, 2020). Each type of radiosonde is subject to known small temperature and

Table 1
Station Number (for Figures), Latitude and Longitude of Each Radiosonde Launch Station, the Time Period Covered in This Study, and the Type of Radiosonde Used at That Station

Number on Figures 1 and 2	Station (latitude, longitude)	Time period of radiosonde data used in this paper	Type of radiosonde deployed
1	Rothera (67.6°S, 68.3°W)	2002–2015	Vaisala
2	Mount Pleasant Airport, Falkland Islands (51.8°S, 58.5°W)	2000–2010	Vaisala
3	King Edward Point, South Georgia (54.3°S, 36.5°W)	2015 (January, June, and part of July only)	Vaisala
4	Halley (75.5°S, 26.5°W)	2002–2013	Vaisala
5	Princess Elisabeth station (71.9°S, 23.3°E)	Summer only: 2014/2015, 2015/2016, 2017/2018, 2018/2019	Graw DFM-09
6	Mawson (67.6°S, 62.9°E)	2000–2018	Vaisala
7	Kerguelen Island (49.2°S, 70.1°E)	2019	Modem M2K2-DC
8	Davis (68.6°S, 77.9°E)	2000–2018	Vaisala
9	Casey (66.3°S, 110.5°E)	2000–2018	Vaisala
10	Dumont D'Urville (66.7°S, 140°E)	2019	Modem M2K2-DC
11	Macquarie Island (54.5°S, 158.9°E)	2000–2018	Vaisala

humidity biases that may require a correction if the raw profiles are to be used (Ingleby, 2017). However, in this study we use perturbations to the data rather than the absolute values of the temperatures; it is unlikely that the results will be affected by these systematic errors; however, the data will still be subject to small random errors.

Seven selected stations are located close to the Antarctic coastline and four are on small islands in the Southern Ocean. It is expected that radiosondes launched from each station will measure a different combination of gravity wave sources due to their location. For example, the island stations are remote, tend to be hilly/mountainous, and are subject to strong storms during the austral winter months; storms and wind flow over hills/mountains can also generate gravity waves (M. J. Alexander & Grimsdell, 2013; Moffat-Griffin et al., 2013). Conversely, Dumont D'Urville is located on Petrel Island and approximately 5 km from the main ice sheet. It is subject to strong katabatic winds, which flow from the Antarctic interior, which can also generate gravity waves (Vignon et al., 2020). It is also expected, from previous studies (Moffat-Griffin et al., 2011, 2013), that those stations close to the Drake Passage will see greater levels of gravity wave activity as this is where the main gravity wave "hotspot" is located. The aim of this paper is to determine if there is a seasonal meridional bias in the horizontal direction of propagation of the gravity waves and thus the resulting energy and momentum flux that is transported in a given direction. Recent work from satellite observations (Hindley et al., 2015, 2019; Wright et al., 2017) has indicated that there is some meridional focusing of gravity waves toward 60°S during the austral winter months higher up in the stratosphere. However, as satellites can only observe part of the gravity wave spectrum, this study will utilize the radiosonde observations of short vertical wavelength gravity waves to determine if this meridional propagation is also present.

3. Analysis Methodology

3.1. Wavelet Analysis

To extract information on gravity wave parameters (e.g., horizontal direction of propagation) from a radiosonde profile, a standard wavelet technique was applied to the data (Moffat-Griffin et al., 2011; Murphy et al., 2014; Zink & Vincent, 2001). A third-order polynomial is fitted to the radiosonde profiles and subtracted from the original profiles, resulting in a residual profile. These residual (perturbation) profiles are analyzed.

To identify individual gravity waves within these perturbation profiles, a technique is used that involves the wavelet transform. This is a proven technique that has been used in many studies of gravity waves in radiosonde data (Moffat-Griffin et al., 2011; Murphy et al., 2014; Zink & Vincent, 2001). First, the application of a Morlet wavelet transform is applied to the wind perturbation profiles. The wavelet coefficients of these profiles are then squared and added together to create a surface space in altitude and vertical wavenumber. In this individual wave regions can be identified (Zink & Vincent, 2001). For each identified wave region, a

reverse wavelet transform (Torrence & Compo, 1998) is then applied. This provides temperature and wind speed perturbation profiles for each identified wave in the profile. These resulting individual wave profiles are analyzed using the dispersion relation, hodograph analysis, and Stokes parameter analysis (Murphy et al., 2014; Vincent et al., 1997; Wang & Geller, 2003). These analyses yield wave parameters, including phase speed, frequency, horizontal and vertical wavelength, and horizontal and vertical direction of propagation.

The analyses show (see Supporting Information Figure S1) that the gravity wave parameters observed exhibit a similar distribution across all stations to those observed previously at Halley (Moffat-Griffin & Colwell, 2017) and Davis (Murphy et al., 2014) using radiosondes. Horizontal wavelengths are in the range 0–800 km, vertical wavelengths 0.2–4 km, and intrinsic frequencies 1*f*–4*f*, where *f* is the Coriolis frequency.

This study focuses only on the upward propagating gravity waves during the austral winter (June, July, and August) and austral summer (December, January, and February).

3.2. Angular Distributions of Wave Energy and Momentum Flux

An angular distribution (also known as a horizontal direction distribution) of gravity wave energy was described in Vincent et al. (1997) and used to examine the dominant direction that gravity wave energy was directed in a given season. This paper will use this technique and focus on the angular distribution of the total energy density (E_T) and total pseudo-momentum flux (F_T) of the gravity waves identified at the different stations during austral winter and summer.

The total energy density of gravity waves can be calculated according to Equation 1 (Allen & Vincent, 1995).

$$E_T = \frac{1}{2}\left(\overline{u'^2} + \overline{v'^2}\right) + \frac{1}{2}\frac{g^2}{N^2}\overline{\hat{T}'^2} \tag{1}$$

The two terms on the right-hand side of Equation 1 correspond to the kinetic and potential energy density, respectively. The terms in Equation 1 are zonal wind perturbation (u'), meridional wind perturbation (v'), normalized temperature perturbation ($\hat{T}'^2$), and the Brunt-Väisälä frequency (N) profile. An overbar signifies averaging over a specific height range. There is a contribution from vertical energy density (that is derived from the vertical velocity, which cannot be directly measured by radiosondes), but this value is normally small so can be neglected for this study (Vincent et al., 1997).

Momentum is transferred to the mean flow when gravity waves break and is an important part of driving atmospheric circulation. Momentum flux is traditionally calculated using the vertical and horizontal velocity perturbations. For radiosondes, which cannot directly measure vertical velocities, estimates of the pseudo-momentum flux can be calculated using the gravity wave polarization relationships between T', u', and v' (Vincent et al., 1997). The zonal pseudo-momentum flux is calculated using Equation 2, where $\hat{T}'_{+90}$ corresponds to the Hilbert transform of the normalized temperature perturbation and ω is the intrinsic frequency. For the meridional pseudo-momentum flux replace u' with v' in Equation 2.

$$F_u = \overline{u'w'} = -\frac{\omega g}{N^2}\overline{u'\hat{T}'_{+90}}\left(1 - \frac{f^2}{\omega^2}\right) \tag{2}$$

In Equation 2 the $\left(1 - \frac{f^2}{\omega^2}\right)$ term is a weighting function that adjusts for the more effective transport of momentum by higher-frequency waves (Gong & Geller, 2010).

The total pseudo-momentum flux is given by Equation 3:

$$F_T = \sqrt{F_u^2 + F_v^2} \tag{3}$$

Once the gravity wave parameters of horizontal direction of propagation, total energy, and momentum flux have been determined for each wave, the angular distributions can be calculated. The horizontal direction of propagation for the gravity waves over each season is binned into 30° angular segments, and the angular distribution of gravity wave energy is calculated using Equation 4, where i refers to the ith bin/segment, E_i is the gravity wave energy total in that bin, and E_T is the total gravity wave energy over the time frame for all bins.

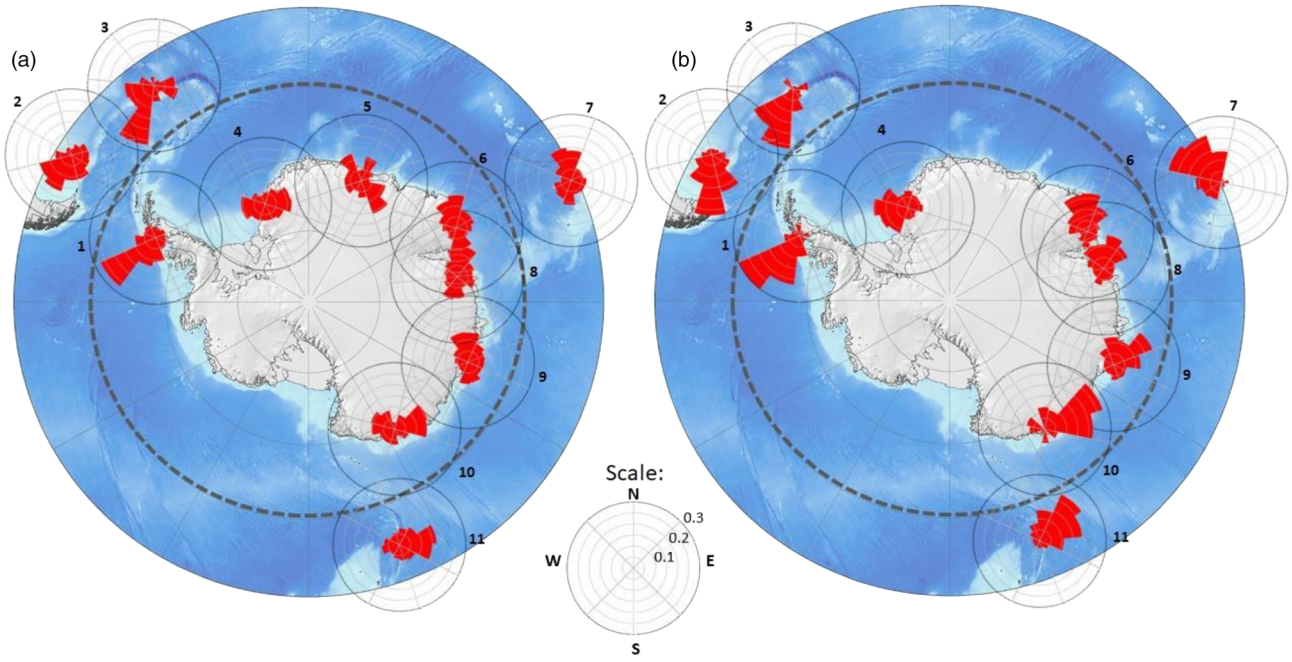

Figure 1. This figure shows the angular distribution of total gravity wave energy density during (a) austral summer (December, January, and February) and (b) austral winter (June, July, and August) for 11 stations (10 during the austral winter). The dashed line indicates 60°S. The scale histogram indicates that the maximum value is 0.3 J kg^{-1} for all histograms. The numbers correspond to the station numbers in Table 1.

For the angular distribution of the absolute pseudo-momentum flux, we use the same method; see Equation 5, where F is the pseudo-momentum flux.

$$\Phi_i = \frac{\sum E_j}{E_T} \tag{4}$$

$$\Phi_i = \frac{\sum F_j}{F_T} \tag{5}$$

4. Results and Discussion

The angular distributions of gravity wave energy density and total pseudo-momentum flux have been calculated for the austral winter and austral summer periods. Figure 1 shows the energy density angular distribution for (a) December, January, and February (austral summer) and (b) June, July, and August (austral winter). Figure 2 is the same but for the pseudo-momentum flux angular distributions. The data are displayed as an angular histogram and are centered over their respective stations location.

During the austral summer the angular distribution of the gravity wave energy density and pseudo-momentum flux measurements over the mainland Antarctic stations (Stations 4–9) are aligned along the eastward and westward axis, with slightly higher value energy density and pseudo-momentum flux heading westward. Dumont D'Urville (Station 10) is the exception to this where a westward and a south-eastward split in the angular distribution is observed. The gravity wave energy density and pseudo-momentum flux measurements over Kerguelen Island (7) and Macquarie Island (12) are similar to those of the mainland stations but with a stronger westward distribution. In the Drake Passage region, the distributions over South Georgia (3) and Rothera (1) stations exhibit strong south-westward and north-westward directions, respectively. The gravity wave energy densities and pseudo-momentum fluxes over both sites are thus directed toward latitudes near 60°S; this is consistent with previous studies (Moffat-Griffin et al., 2011, 2017). The Falkland Islands (3) angular distributions show a westward directionality too, but not as strongly as the two other data sets in the Drake Passage region. The mainland Antarctic data tend to show an angular distribution aligned along the eastward and westward axis, with slightly higher value energy density and pseudo-momentum flux heading westward.

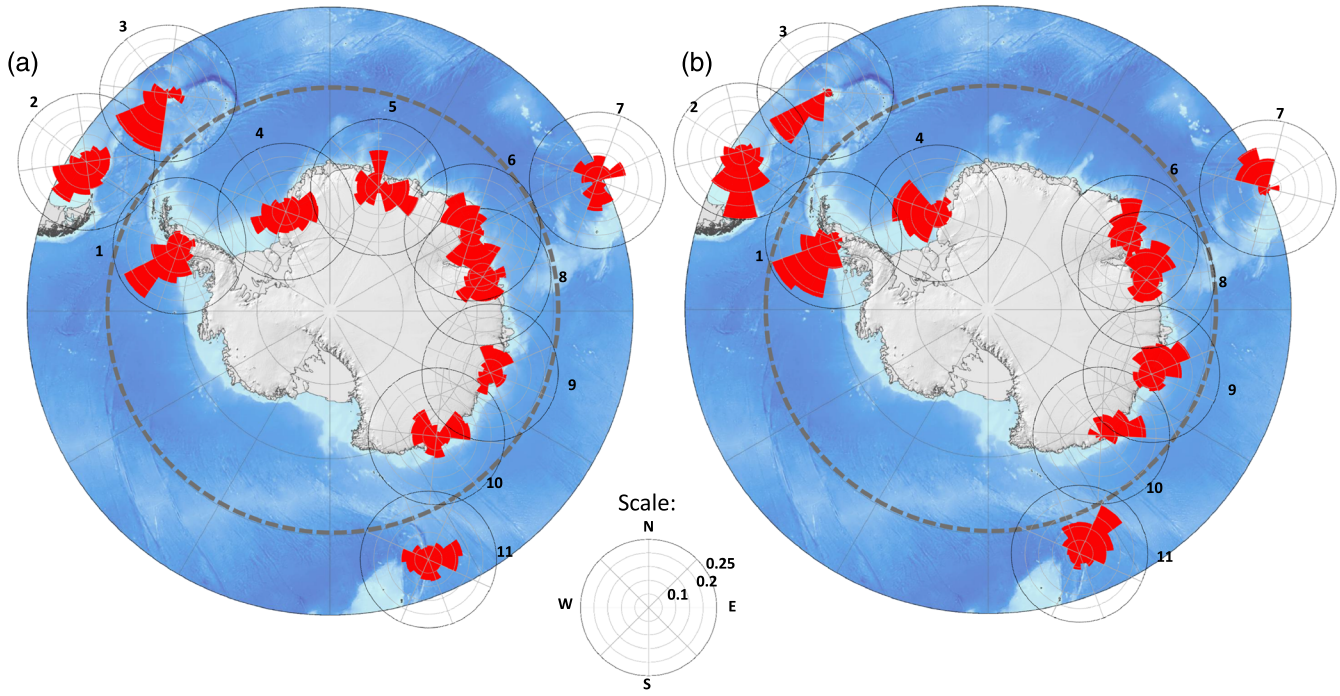

Figure 2. This figure shows same as Figure 1 but for pseudo-momentum flux for 11 stations (10 during the austral winter). The dashed line indicates 60°S. The scale histogram indicates that the maximum value is 0.25 mPa for all histograms.

The range of angular distributions seen during the summer months is likely to be influenced by critical level filtering. In the summer months there are no strong eastward winds, as the Polar Vortex is not present, only weaker eastward winds with a wind reversal occurring typically in the lower stratosphere. These results cover an altitude range of 12 to 30 km which include the wind reversal region.

During the austral winter a clear change in the dominant direction, and magnitudes, of the angular distributions for gravity wave energy density and pseudo-momentum flux is observed. The island stations of Macquarie (11), Kerguelen (7), South Georgia (3), and the Falklands (2) show a clear strong westward to south-westward dominant direction with the maximum values for energy density and pseudo-momentum flux being seen from both the Falkland Islands and South Georgia. The mainland stations (4–10) all show an angular distribution with a clear northwestward to west-northwestward dominance. The Rothera angular distributions show that the north-westward bin dominates. The Drake Passage stations (1–3) show the highest magnitude bins across all the angular distributions.

Those stations South of 60°S tend to show a northwestward-west-northwestward dominance in their distributions, with the stations closer to 60°S showing the largest magnitudes. Those stations to the North of 60°S show a very strong southwestward-west-southwestward directionality in both energy density and pseudo-momentum flux. Even though the directional distributions for both Rothera and South Georgia are similar in both seasons, there will be a greater impact during the austral winter when favorable stratospheric conditions (Moffat-Griffin et al., 2017) mean that these waves are likely to propagate to a higher altitude before they break, thus having a greater impact on stratospheric dynamics during this season.

During the austral winter months, it is expected that there will be a higher level of gravity wave activity as the strong circumpolar eastward jet is present and storms are more frequent and stronger than those during the summer months. Previous studies have also shown that, due to critical level filtering of the gravity waves by the strong eastward winds, it is expected to see more westward propagating waves in the austral winter. What was not fully expected though was the meridional bias seen in the data that means these waves are frequently heading toward 60°S during the winter.

It is expected that these waves will contribute to the hotspot of gravity wave activity around 60°S as these waves tend to have much higher horizontal group velocities compared to their vertical group velocities

(see Supporting Information Figures S1c–S1f). This means they have shallow angles of propagation (Fritts & Alexander, 2003; Murphy et al., 2014) and can travel large horizontal distances before they dissipate.

5. Conclusions

This study examined the horizontal directional distributions of gravity wave energy density and pseudo-momentum flux from 11 Antarctic and sub-Antarctic stations during the austral summer and winter. It is has shown that during the austral winter months there is a greater likelihood of waves propagating toward 60°S and transporting larger pseudo-momentum fluxes and energy densities than during the austral summer months.

This wintertime convergence of gravity waves observed in the lower stratosphere provides strong support for the satellite observations higher up in the stratosphere (S. P. Alexander et al., 2016; Ehard et al., 2017; Hindley et al., 2015). This meridional movement of gravity waves needs to be taken into consideration in future gravity wave parameterization development. Currently, gravity wave parameterizations do not allow for horizontal gravity wave propagation from a source region.

The results in this paper also show, for the first time, that short vertical wavelength gravity waves in the lower stratosphere are propagating meridionally toward 60°S during the austral winter. Incorporating meridional transport into gravity wave parameterizations will help to resolve the hotspot of gravity wave activity in global circulation models and the missing momentum flux in this 60°S region.

Data Availability Statement

Data for the Météo-France stations can be found online (at https://donneespubliques.meteofrance.fr/?fond=produit&id_produit=97&id_rubrique=33). Data from the British Antarctic Survey stations can be found online (at http://catalogue.ceda.ac.uk/uuid/37f2bef57e28bcd780a5cbfe077f4bf8). Data from the Met Office high-resolution radiosonde data from the Falkland Islands can be found online (at http://catalogue.ceda.ac.uk/uuid/c1e2240c353f8edeb98087e90e6d832e). Australian Antarctic Division station data are available on request from the archives held by the Australian Bureau of Meteorology (www.bom.gov.au). Radiosonde data for Princess Elisabeth Antarctica station are available on request via the Royal Meteorological Institute of Belgium (https://www.meteo.be) on the site (http://ozone.meteo.be/meteo/view/en/10666322-Instruments+Antarctica.html).

Acknowledgments

This work was funded by the Natural Environment Research Council on Grant NE/R001235/1 DRAGON-WEX. Wright's time was funded by a Royal Society Research Fellowship, Reference UF160545. We acknowledge the Antarctic operators who have shared their radiosonde data with us for this study. They are British Antarctic Survey, Météo-France, Meteorological Institute of Belgium, and the Australian Antarctic Division. These data would not be possible without the hard work of those Antarctic staff who launch these radiosondes, sometimes in very poor weather conditions! We acknowledge the Royal Meteorological Institute of Belgium and Belgian Science Policy office research project Contracts EA/34/1B and BR/143/A2/AEROCLOUD for providing the radio sounding data at Princess Elisabeth Antarctica station (PEA). In addition, the radio soundings at PEA have been supported by the International Polar Foundation and the Swiss Federal Institute for Forest, Snow and Landscape research. We acknowledge that the Australian Antarctic radiosonde data are sourced from the Australian Bureau of Meteorology.

References

Alexander, M. J. (1998). Interpretations of observed climatological patterns in stratospheric gravity wave variance. *Journal of Geophysical Research*, *103*(D8), 8627–8640. https://doi.org/10.1029/97JD03325

Alexander, M. J., & Barnet, C. (2007). Using satellite observations to constrain parameterizations of gravity wave effects for global models. *Journal of the Atmospheric Sciences*, *64*(5), 1652–1665. https://doi.org/10.1175/jas3897.1

Alexander, M. J., Eckermann, S. D., Broutman, D., & Ma, J. (2009). Momentum flux estimates for South Georgia Island mountain waves in the stratosphere observed via satellite. *Geophysical Research Letters*, *36*, L12816. https://doi.org/10.1029/2009gl038587

Alexander, M. J., & Grimsdell, A. W. (2013). Seasonal cycle of orographic gravity wave occurrence above small islands in the Southern Hemisphere: Implications for effects on the general circulation. *Journal of Geophysical Research: Atmospheres*, *118*, 11,589–11,599. https://doi.org/10.1002/2013JD020526

Alexander, P., Luna, D., Llamedo, P., & de la Torre, A. (2010). A gravity waves study close to the Andes mountains in Patagonia and Antarctica with GPS radio occultation observations. *Annales de Geophysique*, *28*(2), 587–595. https://doi.org/10.5194/angeo-28-587-2010

Alexander, S. P., Klekociuk, A. R., & Tsuda, T. (2009). Gravity wave and orographic wave activity observed around the Antarctic and Arctic stratospheric vortices by the COSMIC GPS-RO satellite constellation. *Journal of Geophysical Research*, *114*, D17103. https://doi.org/10.1029/2009JD011851

Alexander, S. P., Sato, K., Watanabe, S., Kawatani, Y., & Murphy, D. J. (2016). Southern Hemisphere extratropical gravity wave sources and intermittency revealed by a middle-atmosphere general circulation model. *Journal of the Atmospheric Sciences*, *73*(3), 1335–1349. https://doi.org/10.1175/jas-d-15-0149.1

Allen, S. J., & Vincent, R. A. (1995). Gravity wave activity in the lower atmosphere: Seasonal and latitudinal variations. *Journal of Geophysical Research*, *100*(D1), 1327–1350. https://doi.org/10.1029/94JD02688

Ehard, B., Kaifler, B., Dörnbrack, A., Preusse, P., Eckermann, S. D., Bramberger, M., et al. (2017). Horizontal propagation of large-amplitude mountain waves into the polar night jet. *Journal of Geophysical Research: Atmospheres*, *122*, 1423–1436. https://doi.org/10.1002/2016JD025621

Fritts, D. C., & Alexander, M. J. (2003). Gravity wave dynamics and effects in the middle atmosphere. *Reviews of Geophysics*, *41*(1), 1003. https://doi.org/10.1029/2001rg000106

Fritts, D. C., Vadas, S. L., Wan, K., & Werne, J. A. (2006). Mean and variable forcing of the middle atmosphere by gravity waves. *Journal of Atmospheric and Solar-Terrestrial Physics*, *68*(3–5), 247–265. https://doi.org/10.1016/j.jastp.2005.04.010

Garcia, R. R., Smith, A. K., Kinnison, D. E., Cámara, Á. D., & Murphy, D. J. (2017). Modification of the gravity wave parameterization in the whole atmosphere community climate model: Motivation and results. *Journal of the Atmospheric Sciences*, *74*(1), 275–291. https://doi.org/10.1175/jas-d-16-0104.1

Gong, J., & Geller, M. A. (2010). Vertical fluctuation energy in United States high vertical resolution radiosonde data as an indicator of convective gravity wave sources. *Journal of Geophysical Research*, *115*, D11110. https://doi.org/10.1029/2009JD012265

GRAW (2020). https://www.graw.de/products/radiosondes/dfm-09/, edited.

Hendricks, E. A., Doyle, J. D., Eckermann, S. D., Jiang, Q., & Reinecke, P. A. (2014). What is the source of the stratospheric gravity wave belt in austral winter? *Journal of the Atmospheric Sciences*, *71*(5), 1583–1592. https://doi.org/10.1175/jas-d-13-0332.1

Hindley, N. P., Wright, C. J., Smith, N. D., Hoffmann, L., Holt, L. A., Alexander, M. J., et al. (2019). Gravity waves in the winter stratosphere over the Southern Ocean: High-resolution satellite observations and 3-D spectral analysis. *Atmospheric Chemistry and Physics*, *19*(24), 15,377–15,414. https://doi.org/10.5194/acp-19-15377-2019

Hindley, N. P., Wright, C. J., Smith, N. D., & Mitchell, N. J. (2015). The southern stratospheric gravity wave hot spot: Individual waves and their momentum fluxes measured by COSMIC GPS-RO. *Atmospheric Chemistry and Physics*, *15*(14), 7797–7818. https://doi.org/10.5194/acp-15-7797-2015

Hoffmann, L., Grimsdell, A. W., & Alexander, M. J. (2016). Stratospheric gravity waves at southern hemisphere orographic hotspots: 2003–2014 AIRS/Aqua observations. *Atmospheric Chemistry and Physics Discussions*, *2016*, 1–30. https://doi.org/10.5194/acp-2016-341

Hoffmann, L., Xue, X., & Alexander, M. J. (2013). A global view of stratospheric gravity wave hotspots located with Atmospheric Infrared Sounder observations. *Journal of Geophysical Research: Atmospheres*, *118*, 416–434. https://doi.org/10.1029/2012JD018658

Ingleby, B. (2017). *An Assessment of Different Radiosonde Types 2015/2016; ECMWF Technical Memorandum No. 807; European Centre for Medium Range Weather Forecasts*. Reading, UK.

Jackson, D. R., Gadian, A., Hindley, N. P., Hoffmann, L., Hughes, J., King, J., et al. (2017). The south georgia wave experiment: A means for improved analysis of gravity waves and low-level wind impacts generated from mountainous islands. *Bulletin of the American Meteorological Society*, *99*(5), 1027–1040. https://doi.org/10.1175/BAMS-D-16-0151.1

Jiang, Q., Doyle, J. D., Eckermann, S. D., & Williams, B. P. (2019). Stratospheric trailing gravity waves from New Zealand. *Journal of the Atmospheric Sciences*, *76*(6), 1565–1586. https://doi.org/10.1175/jas-d-18-0290.1

Jiang, Q., Reinecke, A., & Doyle, J. D. (2014). Orographic wave drag over the Southern Ocean: A linear theory perspective. *Journal of the Atmospheric Sciences*, *71*(11), 4235–4252. https://doi.org/10.1175/jas-d-14-0035.1

McLandress, C., Shepherd, T. G., Polavarapu, S., & Beagley, S. R. (2012). Is missing orographic gravity wave drag near 60°S the cause of the stratospheric zonal wind biases in chemistry climate models? *Journal of the Atmospheric Sciences*, *69*(3), 802–818. https://doi.org/10.1175/jas-d-11-0159.1

MeteoModem (2020). http://www.meteomodem.com/

Moffat-Griffin, T., & Colwell, S. R. (2017). The characteristics of the lower stratospheric gravity wavefield above Halley (75°S, 26°W), Antarctica, from radiosonde observations. *Journal of Geophysical Research: Atmospheres*, *122*, 8998–9010. https://doi.org/10.1002/2017JD027079

Moffat-Griffin, T., Hibbins, R. E., Jarvis, M. J., & Colwell, S. R. (2011). Seasonal variations of gravity wave activity in the lower stratosphere over an Antarctic Peninsula station. *Journal of Geophysical Research*, *116*, D14111. https://doi.org/10.1029/2010JD015349

Moffat-Griffin, T., Jarvis, M. J., Colwell, S. R., Kavanagh, A. J., Manney, G. L., & Daffer, W. H. (2013). Seasonal variations in lower stratospheric gravity wave energy above the Falkland Islands. *Journal of Geophysical Research: Atmospheres*, *118*, 10,861–10,869. https://doi.org/10.1002/jgrd.50859

Moffat-Griffin, T., Wright, C. J., Moss, A. C., King, J. C., Colwell, S. R., Hughes, J. K., & Mitchell, N. J. (2017). The South Georgia Wave Experiment (SG-WEX): Radiosonde observations of gravity waves in the lower stratosphere. Part I: Energy density, momentum flux and wave propagation direction. *Quarterly Journal of the Royal Meteorological Society*, *143*(709), 3279–3290. https://doi.org/10.1002/qj.3181

Murphy, D. J., Alexander, S. P., Klekociuk, A. R., Love, P. T., & Vincent, R. A. (2014). Radiosonde observations of gravity waves in the lower stratosphere over Davis, Antarctica. *Journal of Geophysical Research: Atmospheres*, *119*, 11,973–911,996. https://doi.org/10.1002/2014JD022448

PDC (2015). http://basmet.nerc-bas.ac.uk/sos/ Polar Data Centre, edited.

Sato, K. (2010). Seasonal variation and sources of atmospheric gravity waves in the Antarctic. *Antarctic Record*, *54*(Sp. Iss. SI), 333–348. https://doi.org/10.15094/00009561

Torrence, C., & Compo, G. P. (1998). A practical guide to wavelet analysis. *Bulletin of the American Meteorological Society*, *79*(1), 61–78. https://doi.org/10.1175/1520-0477(1998)079<0061:APGTWA>2.0.CO;2

Vaisala (2013). RS92-SGP datasheet, edited. http://www.vaisala.com/en/products/soundingsystemsandradiosondes/radiosondes/Pages/RS92.aspx

Vignon, É., Picard, G., Durán-Alarcón, C., Alexander, S. P., Gallée, H., & Berne, A. (2020). Gravity wave excitation during the coastal transition of an extreme katabatic flow in Antarctica. *Journal of the Atmospheric Sciences*, *77*(4), 1295–1312. https://doi.org/10.1175/jas-d-19-0264.1

Vincent, R., Allen, S. J., & Eckermann, E. (1997). Gravity-wave parameters in the lower stratosphere. In K. Hamilton (Ed.), *Gravity wave processes: Their parameterization in global climate models* (pp. 7–25). New York: Springer-Verlag.

Wang, L., & Geller, M. A. (2003). Morphology of gravity-wave energy as observed from 4 years (1998–2001) of high vertical resolution U.S. radiosonde data. *Journal of Geophysical Research*, *108*(D16), 4489. https://doi.org/10.1029/2002JD002786

Whiteway, J. A., & Duck, T. J. (1996). Evidence for critical level filtering of atmospheric gravity waves. *Geophysical Research Letters*, *23*(2), 145–148. https://doi.org/10.1029/95GL03784

Wright, C. J., Hindley, N. P., Hoffmann, L., Alexander, M. J., & Mitchell, N. J. (2017). Exploring gravity wave characteristics in 3-D using a novel S-transform technique: AIRS/Aqua measurements over the Southern Andes and Drake Passage. *Atmospheric Chemistry and Physics*, *17*(13), 8553–8575. https://doi.org/10.5194/acp-17-8553-2017

Wright, C. J., Hindley, N. P., Moss, A. C., & Mitchell, N. J. (2016). Multi-instrument gravity-wave measurements over Tierra del Fuego and the Drake Passage—Part 1: Potential energies and vertical wavelengths from AIRS, COSMIC, HIRDLS, MLS-Aura, SAAMER, SABER and radiosondes. *Atmospheric Measurement Techniques*, *9*(3), 877–908. https://doi.org/10.5194/amt-9-877-2016

Wu, D. L., & Eckermann, S. D. (2008). Global gravity wave variances from Aura MLS: Characteristics and interpretation. *Journal of the Atmospheric Sciences*, *65*(12), 3695–3718. https://doi.org/10.1175/2008jas2489.1

Wu, D. L., & Jiang, J. H. (2002). MLS observations of atmospheric gravity waves over Antarctica. *Journal of Geophysical Research*, *107*(D24), 4773. https://doi.org/10.1029/2002JD002390

Zink, F., & Vincent, R. A. (2001). Wavelet analysis of stratospheric gravity wave packets over Macquarie Island 1. Wave parameters. *Journal of Geophysical Research*, *106*(D10), 10,275–10,288. https://doi.org/10.1029/2000JD900847